mAbs 7:2, 377–389; March/April 2015; Published with license by Taylor & Francis Group, LLC

Improving target cell specificity using a novel monovalent bispecific IgG design

Yariv Mazor[1], Vaheh Oganesyan[1], Chunning Yang[1], Anna Hansen[2], Jihong Wang[3], Hongji Liu[3], Kris Sachsenmeier[4], Marcia Carlson[3], Dhanesh V Gadre[3], Martin Jack Borrok[1], Xiang-Qing Yu[5], William Dall'Acqua[1], Herren Wu[1], and Partha Sarathi Chowdhury[1,*]

[1]Department of Antibody Discovery and Protein Engineering; MedImmune; Gaithersburg, MD USA; [2]Department of Respiratory, Inflammation and Autoimmunity; MedImmune; Gaithersburg, MD USA; [3]Department of Biopharmaceutical Development; MedImmune; Gaithersburg, MD USA; [4]Department of Oncology; MedImmune; Gaithersburg, MD USA; [5]Department of Translational Sciences; MedImmune; Gaithersburg, MD USA

Keywords: Biotechnology, antibody engineering, bispecific antibody, disulfide, multi-targeting, EGFR, HER2, cancer

Abbreviations: IgG, Immunoglobulin G; mAbs, monoclonal antibodies; CH1, 2 and 3-heavy chain constant domain 1, 2 and 3; CL^-, light chain constant domain; CDR, complementarity determining region; RAGE, receptor for advanced glycosylation; IL-6, interleukin 6; EGFR, epidermal growth factor receptor; IGFR, insulin like growth factor receptor; ADCC, antibody-dependent cell-mediated cytotoxicity; FcRn, neonatal Fc receptor; FcγR, receptor for IgG Fc; Q1q, first component of complement 1; PNGase, protein N-glycanase; DSC-differential scanning calorimetry; E:T, ratio of effector to target cells

Monovalent bispecific IgGs cater to a distinct set of mechanisms of action but are difficult to engineer and manufacture because of complexities associated with correct heavy and light chain pairing. We have created a novel design, "DuetMab," for efficient production of these molecules. The platform uses knobs-into-holes (KIH) technology for heterodimerization of 2 distinct heavy chains and increases the efficiency of cognate heavy and light chain pairing by replacing the native disulfide bond in one of the C_H1-C_L interfaces with an engineered disulfide bond. Using two pairs of antibodies, cetuximab (anti-EGFR) and trastuzumab (anti-HER2), and anti-CD40 and anti-CD70 antibodies, we demonstrate that DuetMab antibodies can be produced in a highly purified and active form, and show for the first time that monovalent bispecific IgGs can concurrently bind both antigens on the same cell. This last property compensates for the loss of avidity brought about by monovalency and improves selectivity toward the target cell.

Introduction

The concept of dual targeting, either with antibody combinations or bispecific antibodies, is based on the targeting of multiple disease modifying factors with one drug.[1-6] Advancement in molecular engineering and expression technologies now allows efficient production of bispecific antibodies, which generally offer a simpler development path because pre-clinical and clinical testing can be done with one molecule. Extensive knowledge and infrastructure on developing therapeutic monospecific immunoglobulins (IgGs) have created a trend for IgG-like bispecifics. These molecules are either symmetrical or asymmetrical. The main difference between the 2 is that the former is bivalent, while the latter is monovalent, for each target. The concept of monovalent bispecific IgG is thought to have a unique therapeutic niche [7,8] in that they (i) do not cause receptor homodimerization, (ii) potentially have reduced toxicity on non-target tissues due to loss of avidity for each antigen, and (iii) have better selectivity when both antigens are either selectively restricted or abundantly expressed on target cells.

Asymmetric bispecific molecules are relatively hard to make because they involve heterodimerization of 2 distinct heavy chains and correct pairing of the cognate light chain (LC) and heavy chain (HC). Heterodimerization of the HCs has been addressed by several techniques, such as knobs-into-holes (KIH),[9] electrostatic steering of C_H3,[10] C_H3 strand exchanged engineered domains,[11] and leucine zippers,[12] The pairing of the correct light and heavy chains has been ensured by using one of these HC heterodimerization techniques along with the use of a common light chain,[13] domain cross-over between C_H1 and C_L,[14] coupling of the heavy and light chains with a linker,[15] in vitro assembly of HC-LC dimers from 2 separate monoclonals,[16,17] or interface engineering of the entire Fab domain.[18] A recent report about an epidermal growth factor

*Correspondence to: Partha Sarathi Chowdhury; Email: chowdhuryp@medimmune.com

Submitted: 12/29/2014; Revised: 12/29/2014; Accepted: 01/02/2015

http://dx.doi.org/10.1080/19420862.2015.1007816

receptor (EGFR) and IGFR targeted bispecific antibody employed a single-chain Fab arm where one LC is linked to its corresponding heavy chain by a 32 amino acid linker peptide.[19] Some of these approaches [15,19] deviate significantly from the natural IgG architecture, while the general applicability of others[18] is not yet completely known. The only approach that does not face chain pairing problems and yet yields a natural human IgG-like bispecific is the "two-in-one" technology.[20] However, since it requires extensive engineering of the complementarity-determining regions (CDR), the 2-in-one technology is not a generic design. Moreover, introducing 2 different specificities into the CDRs of one antibody is not only technically challenging but can lead to bivalency for each target. Thus, there is an increasing trend toward development of general and robust approaches for the generation of monovalent bispecific antibodies with native chain structure.[21]

Utilizing the power of the KIH technology for HC heterodimerization, we developed a new technology for enhanced cognate HC and LC pairing for making monovalent bispecific IgGs. The approach, called DuetMab, replaces the native interchain disulfide bond within one of the 2 C_H1-C_L interfaces with an engineered interchain disulfide bond. The DuetMab molecules maintain the structure and developability properties of natural IgGs. We provide herein a comprehensive biochemical, biophysical and functional analysis of one DuetMab directed against EGFR and human epidermal growth factor receptor (HER)2 and another DuetMab against CD4 and CD70 to validate the platform. To the best of our knowledge, we show for the first time, using these 2 different DuetMabs, binding to both antigens on the surface of the same cell.

Results

An engineered disulfide bond in one of the 2 C_H1-C_L interfaces promotes correct HC-LC pairing in DuetMabs

A set of 3 different positions in the C_H1-C_L interface were identified by structural modeling and predicted to favor the formation of a disulfide bond by introduction of a pair of cysteines. The idea was to replace the native disulfide bond in one of the 2 C_H1-C_L interfaces with the engineered disulfide bond while leaving the wild type disulfide bond in the other Fab arm unchanged. Three different position pairs were tested for engineering the new disulfide bond. One of the 3 was found to promote nearly 100% monovalent bispecific IgG formation (**Table 1**). This variant had F^{126} in the HC and S^{121} in the LC substituted to cysteine (HC: $F^{126}C$/LC: $S^{121}C$) and was selected for making monovalent bispecific IgGs termed DuetMabs (**Fig. 1**). The HCs and LCs used for this study were specific for interleukin-6 (IL-6) and receptor for advanced glycation endproducts (RAGE). The efficiency of correct heavy and light chain pairing was determined by AlphaLISA using reference standard and benchmark bispecific samples. When wild-type anti-RAGE and anti-IL-6 antibodies are co-transfected and co-expressed, 4 different IgGs should in theory be formed, all of which can be purified by a protein A affinity matrix. Our reference standard was the material that theoretically should have about 12.5% correctly assembled monovalent bispecific IgG.[4] When this reference standard was sequentially purified using an IL-6 and RAGE affinity matrix, we got a pure preparation of monovalent bispecific IgG. This material served as our benchmark, and the AlphaLISA signal obtained with it was used to set a reference of nearly 100% bispecificity (**Table 1**). Therefore, cysteine-engineered variants that showed improved AlphaLISA signal over the reference standard and approaching that of the benchmark indicated better pairing of cognate heavy and light chains.

Table 1. Bispecificity of antibody formats to IL-6 and RAGE antigens

Antibody	% bispecificity
Reference standard	14 ± 1.9
Benchmark	100 ± 4.2
KIH bispecific	26 ± 2.3
Variant 1: HC $A^{141}C$, LC $F^{116}C$	39 ± 4.8
Variant 2: HC $H^{168}C$, LC $T^{164}C$	35 ± 2.7
Variant 3: HC $F^{126}C$, LC $S^{121}C$	98 ± 3.6

Bispecificity was determined by AlphaLISA. The % bispecificity and the ± s. d. represents the mean value of triplicate reads. Reference standard refers to the purified IgG from a co-transfection of wild type anti-IL-6 and anti-RAGE. Benchmark refers to the IgG obtained after after 2 step affinity chromatography of the reference standard over IL-6 and RAGE matrix. KIH bispecific refers to the IgG obtained by co-transfection of anti-IL-6 and anti-RAGE containing the hole and knob mutations in the CH3, respectively. Variant 1, 2 and 3 have hole mutations in the anti-IL-6 C_H3 and knob mutations in anti-RAGE C_H3. All three variants antibodies have wild type C_H1-C_L interface for the anti-IL-6 arm but differ in the mutations in the C_H1-C_L interface of the anti-RAGE arm as follows: Variant 1: HC $A^{141}C$, LC $F^{116}C$; Variant 2: HC $H^{168}C$, LC $T^{164}C$ and Variant 3: HC $F^{126}C$, LC $S^{121}C$. Variant 3 was used to make DuetMabs. The positions for the new pair of cysteines remains the same for both kappa (κ) and lambda (λ) constant domains. Numbering is according to Kabat [Sequences of Proteins of Immunological Interest, 5th Ed. Public Health Service, National Institutes of Health, Bethesda, MD (1991)].

Physico-chemical characterization of purified EGFR-HER2 DuetMab show correct pairing between heavy and light chains

DuetMabs composed of cetuximab and trastuzumab (EGFR-HER2 DuetMab) and CD4-CD70 were produced by transient co-transfection of HEK293F cells with equimolar concentration of 2 plasmids, the pDuet-Heavy and pDuet-Light vectors as described in the Materials and Methods. The antibody titer for the EGFR-HER2 DuetMab was 150 mg/l, while that for cetuximab and trastuzumab were 90 mg/l and 200 mg/l, respectively. Likewise, the titer for CD4-CD70 DuetMab was 193 mg/l while that of the CD4 and CD70 parental mAbs were 241 and 209 mg/l, respectively. Thus antibody titers for both the DuetMabs correlated well with the expression levels of the 2 parental IgGs. DuetMabs were purified using standard protein A chromatography. Purity and chain composition were determined by sodium dodecyl sulfate polyacrylamide gel electrophoresis (SDS-PAGE), analytical size exclusion chromatography (SEC), reversed-phase high performance liquid chromatography (RP-HPLC), and electrospray ionization mass spectrometry (ESI-MS).

By SEC, both, EGFR-HER2 DuetMab (**Fig 2A**) and CD4-CD70 DuetMab (**Fig. S1A**) showed a single peak with very low levels of aggregates and no fragments or free chains. The peaks for each DuetMab was similar to those for the parental molecules (result not shown). The EGFR-HER2 and CD4-CD70 DuetMabs had molecular masses similar to that of whole IgG. The expected and measured intact mass of the EGFR-HER2 DuetMab was 144,986 Da (**Fig. 2B**) and that of the CD4-CD70 DuetMab was 145,650 Da (**Fig. S1B**) as determined by reversed-phase liquid chromatography-mass spectrometry (RP-HPLC-MS). In comparison, the mass of cetuximab and trastuzumab was found to be 145,032 Da and 145,224 Da, respectively and that of anti-CD4 and anti-CD70 were 146,551 Da and 144,973 Da, respectively (result not shown). No free heavy and light chains were detected by RP-HPLC.

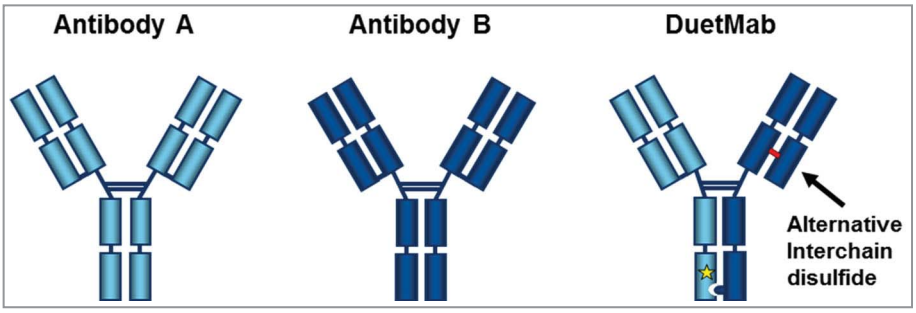

Figure 1. Schematic diagram to differentiate conventional monospecific mAbs (antibodies A and B) from DuetMab. Heterodimerization of distinct heavy chains is achieved by use of the KIH technology. The DuetMab is comprised of one wild-type Fab and one engineered Fab with the interchain disulfide redesigned (in red) within the C_H1-C_L interface. The yellow star on the hole heavy chain represent the RF mutation to ablate protein A binding.

The EGFR-HER2 DuetMab is composed of 4 different chains. **Figure 2C** shows the chain composition and electrophoretic profile of EGFR-HER2 DuetMab and **Fig. S1C** shows the same for CD4-CD70 DuetMab. Under non-reducing RP-HPLC, the intact EGFR-HER2 DuetMab eluted as a single peak at 27.7 min (**Fig. 2C**), which was intermediate between cetuximab (28.9 min) and trastuzumab (26.4 min) (result not shown). Free heavy and light chains were not detected. Under reducing conditions, the DuetMab separated into 4 stoichiometric fractions, corresponding to the 4 chains comprising the molecule. The retention times of the heavy and light chains of the DuetMab were similar to the retention time for the heavy and light chains of the 2 parental IgGs (cetuximab HC: 20.3 min and LC: 15.6 min; trastuzumab HC: 18.1 min and LC: 14.3 min). Similar observations were made for the CD4-CD70 DuetMab (**Fig. S1C**). Under non-reducing conditions the DuetMab eluted as a single peak at 25.9 minute compared to anti-CD4 and anti-CD70 eluting at 25.7 and 26.2 minutes, respectively (result not shown). Under reducing conditions the DuetMab separated into 4 stoichiometric fractions, corresponding to the 4 chains comprising the molecule (**Fig. S1C**). The retention times of the heavy and light chains of the DuetMab were similar to the retention time for the heavy and light chains of the 2 parental IgGs (anti-CD4 HC: 9.1 min and LC: 6.4 min; anti-CD70 HC: 9.6 min and LC: 6.2 min).

Peptide mapping showed that all predicted inter-chain disulfide bonds were formed and there was no disulfide scrambling between heavy and light chains of EGFR-HER2 DuetMab (**Fig. 2D** and **Table S1**) and CD4-CD70 DuetMab (**Fig. S1D** and **Table S2**). As indicated by red arrows in **Figure 2D**, 2 peptides eluting at 9.6 min and 41.4 min were identified as the disulfide-linked light and heavy chain pair of cetuximab (designated as X) and trastuzumab (designated as Y) Fab arms. No peptides corresponding to non-cognate chain pairing were identified. The blue arrow indicates peptide fragment resulting from heterodimerization of the 2 different heavy chains. No peptide representing a homodimerized Fc was found. Under reducing conditions only peaks corresponding to disulfide bond-containing peptides disappeared (result not shown). Similar observations were made for the CD4-CD70 DuetMab. We have also measured the amount of free cysteines in the EGFR-HER2 DuetMab and found that only about 0.3% free cysteine is detected in the engineered Fab arm (**Table 2**). The sensitivity of our assay system is thus below 1%, and any significant chain mispairing would have been detected in the peptide mapping analysis. Pairing of cognate heavy and light chains was also confirmed by LC-MS analysis of fragments generated by papain digestion of the 2 DuetMabs. As shown in **Figure 2E**, the EGFR-HER2 DuetMab generated 3 distinct fragments, one corresponding to the KIH-linked cetuximab-trastuzumab hybrid Fc and 2 Fabs. Of these, one Fab corresponded to the cetuximab Fab and the other to the trastuzumab Fab. In contrast, each of the 2 parental antibodies had only one

Table 2. Free cysteine analysis of EGFR-HER2 DuetMab

Disulfide-bond linkages	Cysteines	% Free thiols
L-H (X) (WT)	LC Cys214	ND
L-H (Y) (Mut)	LC Cys121	0.20%
	HC Cys 126	0.35%
H(X) - H(Y) Stabilizing disulfide-bond	HC Cys349	0.92%
	HC Cys354	0.53%
C_H3 (X) hole	HC Cys367	0.84%
	HC Cys425	0.69%
	HC Cys367	5.14%
C_H3 (Y) knob	HC Cys425	6.50%
Hinge (H-H)	HC Cys 226,229	0.49%

X indicates cetuximab- and Y indicates transtuzumab-derived peptides. Only inter-chain and the engineered intra-chain disulfide bond-linked cysteines in the CH3 domain are shown. Free thiols are capped using N-ethylmalimide (NEM) before Lys-C digestion. The percentage of free cysteines were calculated using selected ions of Cysteine containing peptides with NEM addition divided by the selected ions of reduced peptides. As low as 0.2% free thiol or disulfide-bond scrambling can be detected.

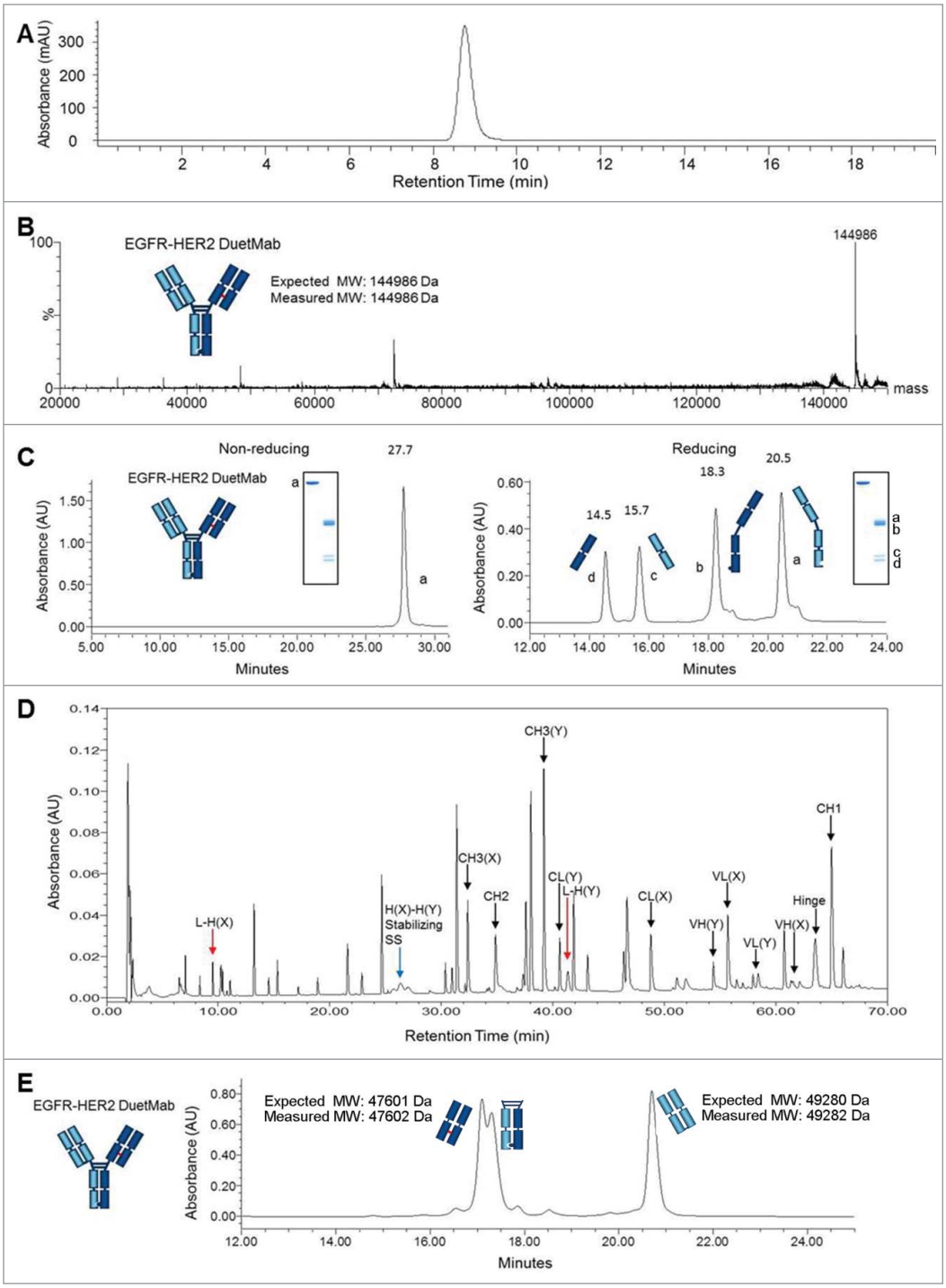

Figure 2. Physico-chemical characterization of purified EGFR-HER2 DuetMab. (**A**) Analytical size-exclusion chromatogram of intact EGFR-HER2 DuetMab. (**B**) Overlay of deconvoluted MS. Indicated is the theoretical and measured mass of intact EGFR-HER2 DuetMab after delglycosylation. (**C**) RP-HPLC and SDS-PAGE analysis. Under non-reducing conditions, EGFR-HER2 DuetMab migrates as an intact molecule with a single elution peak. Under reducing conditions, EGFR-HER2 DuetMab elutes in 4 stoichiometric fractions corresponding to the 2 heavy and 2 light chains. Numbers represent the retention time in minutes for each peak and lowercase letters represent the migration profile of the corresponding peak in SDS-PAGE. (**D**) Non-reduced UV trace of peptide mapping of EGFR-HER2 DuetMab after Lys-C digestion and analysis by LC-MS. The half antibody comprised of the anti-EGFR is referred as (X) while the half antibody comprised of the anti-HER2 is referred as (Y). The peaks corresponding to expected disulfide-linked peptides of C_H1-C_L are labeled in red arrows. The disulfide linked C_H3 peptide is labeled in blue arrow. No peptide corresponding to non-cognate chain pairing were found (more detail in **Table 2**). (**E**) RP-HPLC analysis of papain digested EGFR-HER2 DuetMab. DuetMab eluted in 3 stoichiometric fractions corresponding to the heterodimeric Fc and 2 differentiated Fabs.

Fc and one Fab (data not shown). Similar observations were made for the CD4-CD70 DuetMab (**Fig. S1E**).

DuetMab folds like wild-type Fab

The structure of the DuetMab Fab was solved by x-ray crystallography (**Fig. 3**) to confirm the formation of a new disulfide bond between C^{126} of C_H1 and C^{121} of C_L and to assess whether the disulfide engineering had any effect in the folding of the Fab domain. Crystals of the DuetMab Fab diffracted to 2.1 Å resolution and the structure was solved by molecular replacement using Phaser[22] from CCP4 suite.[23] Trastuzumab Fab (PDB entry 1N8Z, ref.[24]) was used as the template for molecular replacement. 1N8Z Fab is highly homologous to the DuetMab Fab differing in only 4 amino acids corresponding to the engineered cysteines and removal of the wild type disulfide bond. Within the V_H-V_L and C_H1-C_L domains of trastuzumab and DuetMab Fab the Cα backbone showed root mean squared (RMS) deviations of 0.4 Å and 0.5 Å, respectively. Data statistics are presented in (**Table S3**). This crystal structure suggests that the engineered disulfide bond and the absence of a conventional one

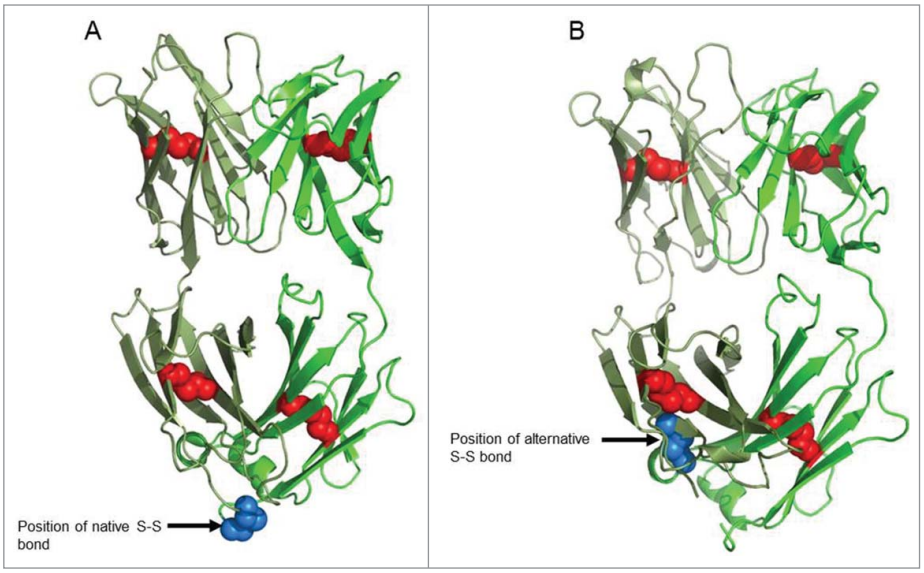

Figure 3. Crystal structure of DuetMab Fab. (**A**) Structure of trastuzumab Fab. Red spheres depict the native intrachain disulfide bonds and blue spheres indicate the native interchain disulfide in C_H1-C_L interface. (**B**) Structure of DuetMab Fab. Red spheres depict the native intrachain disulfide bonds and blue spheres indicate the new disulfide bond between C^{126} of the HC and C^{121} of the LC.

did not change the overall structure of the DuetMab Fab domain. The electron density map confirmed the creation of a new disulfide bond at the location of the newly introduced cysteine residues.

Differential scanning calorimetric study of the EGFR-HER2 DuetMab and the parental antibodies was performed to assess the overall stability of the IgGs. As shown in **Figure 4A**, the 2 parental IgGs, trastuzumab and cetuximab had different onset of unfolding temperatures ($T_{m,\ onset}$) of 60°C and 53°C, respectively, and showed markedly different T_m profile. In comparison, the DuetMab exhibited a T_m profile that was intermediate between the 2 parents and showed a $T_{m,\ onset}$ of 55°C. This is in contrast to the unfolding of the wild type and disulfide engineered Fab where we see the latter to have 9.5°C lower T_m (result not shown). We have also measured the $T_{m,\ onset}$ of the anti-CD4, anti-CD70 antibodies and the corresponding DuetMab and found the $T_{m,\ onset}$ to be 62°C, 61°C and 58°C, respectively (**Fig. 4B**) indicating that the engineered disulfide bond does not significantly affect the $T_{m,\ onset}$ of the whole DuetMab molecules.

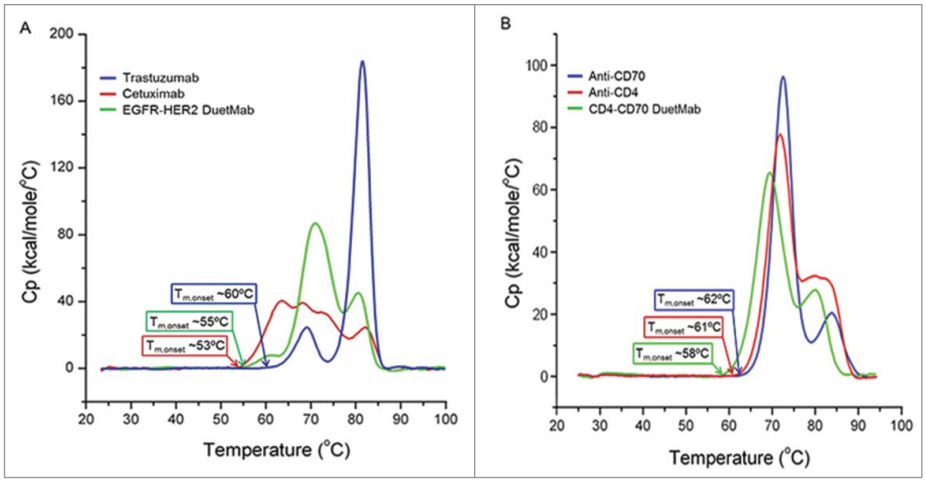

Figure 4. Differential scanning calorimetry profiles of DuetMabs. DSC traces of (**A**) trastuzumab (blue), cetuximab (red), and EGFR-HER2 DuetMab (green) as well as (**B**) anti-CD70 (blue), anti-CD4 (red) and CD4-CD70 DuetMab (green) are shown with the $T_{m,onset}$ of each molecule. The $T_{m,onsets}$ for DuetMabs are similar to the lowest $T_{m,onset}$ of the parental antibodies.

DuetMab can concurrently bind to 2 antigens and show improved cell selectivity by binding 2 antigens on the same cell

When captured on an anti-Fc biosensor, the DuetMab was able to bind both HER2 and EGFR simultaneously (**Fig. 5A**). Concurrent binding was also seen when biotinylated forms of HER2 and EGFR antigens were immobilized on separate streptavidin biosensors and then sequentially exposed to the DuetMab and the other antigen (**Fig. 5B, C**). In both orientations, the DuetMab demonstrated simultaneous binding to both antigens while the parental anti-EGFR and anti-HER2 IgGs exhibited specific binding only to their respective antigen.

Single cell flow cytometry was used to study cell selectivity by 2 separate DuetMabs. The anti-CD4-anti-CD70 DuetMab was used to study specificity for cells that differentially co-express the 2 antigens. We showed that this DuetMab can preferentially bind to a population of T cells co-expressing CD4 and CD70 in a mixture that also contains $CD4^+CD70^-$ T-cells and $CD4^-CD70^+$ B-cells (**Fig. 6A**). To prove that this preferential binding was due to increased avidity conferred by concurrent engagement of both antigens, we used fluorescent dye labeled soluble CD4 (sCD4) and soluble CD70 (sCD70) to detect free antigen binding sites on the DuetMab bound to a cell. As measured by an anti-Fc reagent, the DuetMab bound to double- and single-positive cells in a dose-dependent manner (**Fig. 6B, C**). On double-positive cells very little sCD4 and almost no sCD70 binding was detected (**Fig. 6B, C** red triangle). On the $CD4^-CD70^+$ cell, sCD4 showed an increase in binding with an increasing dose of DuetMab (**Fig. 6B**, green square), but there was no detectable binding by sCD70 (not

Table 3. Receptor density analysis

Cell-line	EGFR	± s.d	HER2	± s.d
A431	83.3×10^4	5.2×10^4	3.3×10^4	0.15×10^4
SK-OV3	14.4×10^4	0.7×10^4	34.5×10^4	1.4×10^4
SKBr3	4.2×10^4	0.3×10^4	176×10^4	7.2×10^4

Quantitative receptor density analysis was determined by QIFIKIT. Cells were incubated with anti-EGFR mouse mAb or anti-HER2 mouse mAb at saturating concentrations of 10 μg/ml followed by labeling with AlexaFluor®488 -conjugated goat anti-mouse IgG F(ab)2 at 20 μg/ml. Optimal primary and secondary antibody concentrations were determined by titration. QIFIKIT Bead standards coated with defined amounts of anti-CD5 mouse mAb were labeled in same manner and were used for the generation of a calibration curve. The receptor density values and the ± s.d. represent the mean value of duplicate reads.

shown). Conversely, in the $CD4^+CD70^-$ cells, sCD70 showed increased binding with increasing dose of the DuetMab (**Fig. 6C**, blue circle), but sCD4 showed no binding (not shown). The degree of DuetMab binding to the 3 different cell types varied from donor to donor or from one cell line to another but it was always much stronger on the $CD4^+CD70^+$ double positive cell and this binding was due to engagement of the DuetMab to both antigens on the same cell (**Fig. S5A**).

We also tested the ability of a DuetMab for preferential binding to cells in a mixture where the 2 antigens are co-expressed at different levels on different cells. We showed that the EGFR-HER2 DuetMab bound better to cells that enabled both arms of the DuetMab to bind antigen, thereby creating an avidity effect. Between A431 ($EGFR^{Hi}HER2^{Low}$; receptor numbers: $83.3 \times 10^4 \pm 5.2 \times 10^4$ and $3.3 \times 10^4 \pm 0.15 \times 10^4$), SK-OV3 ($EGFR^{Med}HER2^{Med}$; receptor numbers: $14.4 \times 10^4 \pm 0.7 \times 10^4$ and $34.5 \times 10^4 \pm 1.4 \times 10^4$) and SKBr3 ($EGFR^{Low}$-$HER2^{Hi}$; receptor numbers: $4.2 \times 10^4 \pm 0.3 \times 10^4$ and $176 \times 10^4 \pm 7.2 \times 10^4$) cells, SK-OV3 has the least number of total binding sites (**Table 3**), yet it shows preferential binding by EGFR-HER2 DuetMab (**Fig. 6D**). This preferential binding is determined by the number of the lower-expressing antigen. In case of SK-OV3, this number is about 14.4×10^4 compared to 3.3×10^4 and 4.2×10^4 for A431 and SKBr3, respectively. To prove this we used biotinylated EGFR and HER2 to detect free binding sites on cell bound EGFR-HER2 DuetMab. The DuetMab bound preferentially to SK-OV3 (**Fig. 6D**, red triangle), which are $EGFR^{Med}HER2^{Med}$. Very little binding by the soluble antigens was detected (**Fig. 6E, F** red triangle), indicating that both arms of the DuetMab are bound to the cell. On SKBr3 ($EGFR^{Low}HER2^{Hi}$, green square in **Fig. 6D-F**) and A431 ($EGFR^{Hi}HER2^{Low}$, blue circle in **Fig. 6D–F**) cells, binding of sEGFR (**Fig. 6E**) and sHER2 (**Fig. 6F**), respectively, increased with increasing DuetMab concentrations. In contrast the binding of sHER2 and sEGFR on SKBR3 and A431, respectively, did not show a strong binding with increasing dose (**Fig. 6E** blue circle and 6F green box). These results indicate that on SK-OV3 the DuetMab engaged in bivalent binding by both the EGFR- and HER2-binding arms, but a significant portion of the DuetMab was bound monovalently by the HER2-binding arm on SKBr3 and by the EGFR-binding arm on A431. The magnitude of EGFR-HER2 DuetMab binding to the 3 different cells varied from one experiment to another but it was always stronger on SK-OV3 compared to SKBr3 and A431 and this strong binding was due to the engagement of both antigens on the surface of SK-OV3 cells (**Fig. S5D**). These results suggests that DuetMabs can engage 2 antigens on the same cell and thereby have better specificity for the target cell.

EGFR-HER2 DuetMab retain antigen and Fc receptor binding kinetics of the parental antibodies

The binding kinetics of the EGFR-HER2 DuetMab to the 2 antigens were determined by Octet analysis. Antibodies were captured on an anti-Fc sensor chip to allow analysis of a 1:1 interaction between antibody and antigen. As shown in **Table 4** and **Fig. S2** the binding kinetics of the DuetMab to each antigen were similar to the parental IgGs for their respective antigens. The binding affinity of the EGFR-HER2 DuetMab to various human Fcγ receptors, FcRn, and C1q was determined by steady-

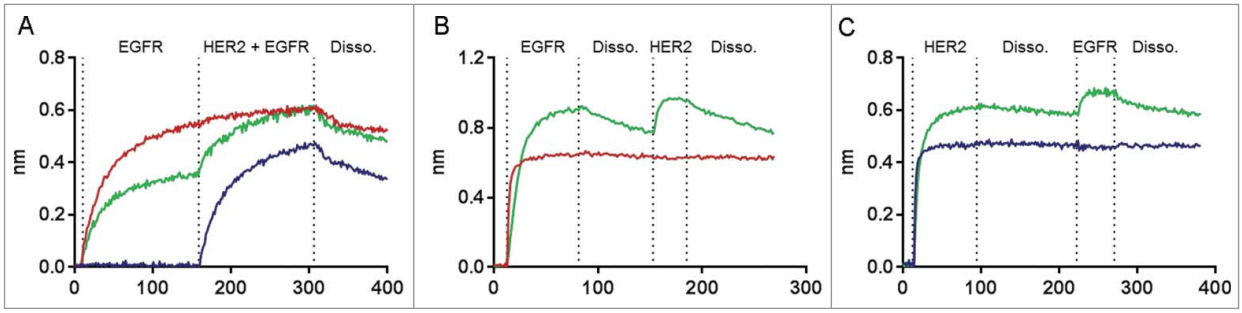

Figure 5. Concurrent binding to EGFR and HER2 by EGFR-HER2 DuetMab as determined by Octet analysis. (**A**) Simultaneous binding using antibody captured format. Traces of EGFR-HER2 DuetMab (green), anti-EGFR (red) and anti-HER2 (blue) represent sequential association interactions first with EGFR then with HER2 followed by terminal dissociation. (**B**) Simultaneous binding using antigen capture format. Sensors loaded with EGFR antigen exposed to successive association and dissociation interactions first with EGFR-HER2 DuetMab (green) and anti-EGFR (red) then with HER2 antigen. (**C**) Simultaneous binding using antigen capture format. Sensors loaded with HER2 antigen exposed to successive association and dissociation interactions first with EGFR-HER2 DuetMab (green) and anti-HER2 (blue) then with EGFR antigen. In both formats the parent antibodies exhibited a single interaction only in response to binding their respective antigen while the EGFR-HER2 DuetMab exhibited binding interactions in response to both EGFR and HER2 antigens.

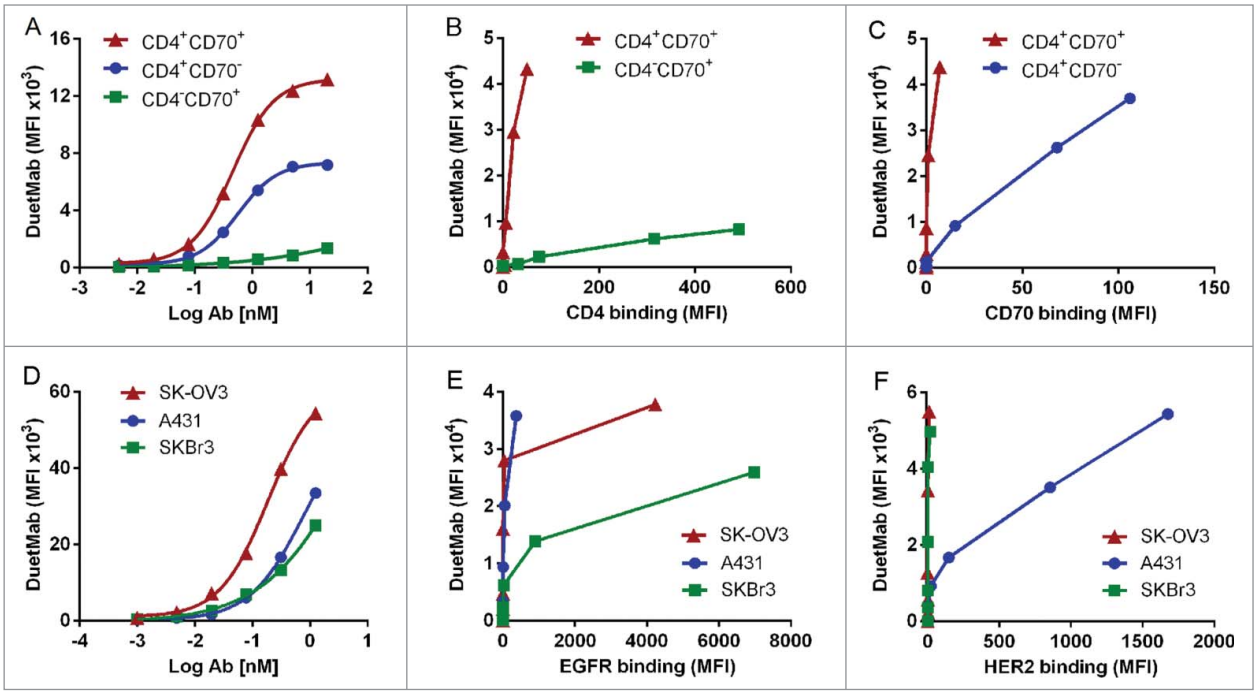

Figure 6. Concurrent binding of DuetMab to 2 antigens on the same cell as determined by FACS analysis. (**A**) Preferential binding by concurrent engagement to 2 antigens (CD4 and CD70) on a single cell as determined by flow-cytometry. Cell-bound DuetMab was detected with PE-labeled anti-human Fc_{γ}. Binding of CD4-CD70 DuetMab to 1:1:1 premix of $CD4^{+}CD70^{+}$ (red triangle), $CD4^{-}CD70^{+}$ (green square) and $CD4^{+}CD70^{-}$ (blue circle) lymphocytes labeled with different tracer dyes. (**B**) Detection of total DuetMab binding (y-axis) and of free CD4 binding sites on cell bound anti CD4-anti CD70 DuetMab using biotin labeled sCD4 (x-axis). (**C**) Detection of total DuetMab binding (y-axis) and of free CD70 binding sites on cell bound anti CD4-anti CD70 DuetMab using biotin labeled sCD70 (x-axis). Each point in (**B**) and (**C**) refers to a different DuetMab concentration. These were 0, 0.001, 0.005, 0.02, 0.08, 0.3 and 1.25 nM. (**D**) Preferential binding of EGFR-HER2 DuetMab to SK-OV3 in a 1:1:1 premix of SK-OV3 ($EGFR^{Med}HER2^{Med}$ in red triangle, SKBr3 ($EGFR^{Low}$-$HER2^{Hi}$ in green square) and A431($EGFR^{Hi}HER2^{Low}$ in blue circle) cells, each labeled with different tracer dyes. The number of EGFR and HER2 sites, respectively, on the 3 cells as determined by QIFIKIT are as follows. A431- $83.3 \times 10^4 \pm 5.2 \times 10^4$ and $\mathbf{3.3 \times 10^4} \pm 0.15 \times 10^4$; SK-OV3 – $\mathbf{14.4 \times 10^4} \pm 0.7 \times 10^4$ and $34.5 \times 10^4 \pm 1.4 \times 10^4$; and SKBr3- $\mathbf{4.2 \times 10^4} \pm 0.3 \times 10^4$ and $176 \times 10^4 \pm 7.2 \times 10^4$. The maximum number of bivalent binding possible on each cell line is indicated in bold. (**E**) Detection of total DuetMab binding (y-axis) and of free EGFR binding sites on cell bound EGFR-HER2 DuetMab using biotin labeled sEGFR (x-axis). (**C**) Detection of total DuetMab binding (y-axis) and of free HER2 binding sites on cell bound EGFR-HER2 DuetMab (x-axis). Each point in (**E**) and (**F**) refers to a different DuetMab concentration. These were 0, 0.02, 0.08, 0.3, 1.25 and 5 nM. Binding of DuetMab was monitored by PE labeled anti-human Fc and binding of biotinylated soluble ligands were monitored by BV421 labeled streptavidin.

state equilibrium binding assay on ProteOn. As shown in **Table 5** and **Fig. S3** the binding kinetics of the DuetMab for the different Fcγ receptors and C1q are indistinguishable from the 2 parental antibodies and NMGC, an isotype control human IgG1. The binding to human and cynomolgus FcRn at pH 6 was indistinguishable and no binding was evident at pH 7.4.

Table 4. Binding kinetics of EGFR-HER2 DuetMab and parental IgGs

Antibody	Antigen	k_{on} (M^{-1} sec^{-1})	k_{off} (sec^{-1})	K_D (nM)
Anti-EGFR IgG	EGFR	1.8×10^5	1.9×10^{-3}	10.3
Anti-HER2 IgG	HER2	2.3×10^5	2.6×10^{-4}	1.1
EGFR-HER2 DuetMab	EGFR	1.7×10^5	2.0×10^{-3}	11.7
	HER2	2.1×10^5	2.8×10^{-4}	1.4

Kinetic measurements to EGFR and HER2 antigens were measured by biolayer interferometry on an Octet384 instrument. The equilibrium dissociation constants, K_D, were calculated as the ratio of k_{off}/k_{on} from a non-linear fit of the data.

EGFR-HER2 DuetMab mimics parental antibodies in cell viability, antibody-dependent cell-mediated cytotoxicity and anti-tumor activity

The biological activity of the EGFR-HER2 DuetMab was compared to the parental antibodies, the monovalent forms of the parental antibodies and combination of the 2. Its effect on the viability of NCI-H358 cells was comparable to a combination of the 2 parental mAbs and significantly more potent than the activity of each (**Fig. 7A**). The same result was observed when SK-OV3 cells were used (data not shown). The EGFR-HER2 DuetMab induced antibody-dependent cell-mediated cytotoxicity (ADCC) in SK-OV3 cells with the same potency as trastuzumab, which was most active compared to cetuximab or the monovalent forms of each (**Fig. 7B**). In the NCI-H358 xenograft model, the EGFR-HER2 DuetMab demonstrated significantly better tumor growth inhibition when compared with the isotype control NMGC IgG or the EGFR-NMGC and HER2-NMGC control DuetMabs and showed similar activity to the combination of the 2 monovalent antibodies (**Fig. 7C**). These results

Table 5. Equilibrium binding of EGFR-HER2 DuetMab and parental IgGs to various Fc receptors

	Antibody K_D (nM)						
Ligand	**FcγR Ia**	**FcγR IIa**	**Fcγ RIIb**	**Fcγ RIIIa (158F)**	**Fcγ RIIIa (158V)**	**C1q**	**Hu FcRn (pH 6)**
EGFR-HER2 DuetMab	7.9	960	5390	2540	315	174	1050
Anti-EGFR	7.1	1000	4640	2440	284	120	1100
Anti-HER2	8.1	903	5620	2270	253	83.3	998
Human IgG1 isotype	9.9	906	5650	2210	246	28.9	810

Kinetic measurements were performed on a surface plasmon resonance-based ProteOn biosensor using steady-state equilibrium binding assay.

suggest that the EGFR-HER2 DuetMab retains the activity of the combination of 2 parents or of the better of the 2 parental antibodies.

DuetMab has similar pharmacokinetics to natural IgG

Severe combined immune deficiency (SCID) mice and human FcRn transgenic mice were used to determine the pharmacokinetic profile of the EGFR-HER2 DuetMab and parental IgGs. All samples had half-lives of ~11 days for the SCID model and ~2 days for the human FcRn transgenic model (**Table 6** and **Fig. S4**). The faster clearance in human FcRn transgenic compared to SCID mice carrying wild-type mouse FcRn is likely due to lower overall expression of the transgene[25] and the higher affinity of mouse FcRn for human IgG.[26]

Discussion

DuetMab is a monovalent bispecific design consisting of 2 different heavy and light chains. Pairing of cognate chains is ensured by replacing the native C_H1-C_L interchain disulfide bond of one of the Fab arms with an engineered disulfide bond and combining this in the context of KIH in the C_H3 domain. We showed that DuetMab preserves the major properties of natural IgG and, further, by binding to 2 targets on the same cell, it compensates for the loss of avidity that can arise because of monovalency for each antigen.

The DuetMab composed of 2 marketed mAbs, anti-EGFR (cetuximab) and anti-HER2 (trastuzumab), descri-bed here demonstrates the feasibility of the platform. Targeting both antigens is important because co-expression of EGFR and HER2 in cancers confers a poor prognosis,[27,28] and the 2 pathways are known to be bypassed in monotherapy.[29] A growing number of in vitro and in vivo studies suggest that dual inhibition of these receptors have therapeutic benefits.[30-32] Through a variety of biophysical, biochemical and biological assays, we conclude that the EGFR-HER2 DuetMab exhibits properties similar to trastuzumab and cetuximab or a combination of the 2. This is valuable because developing a single drug substance such as a DuetMab is generally simpler than a cocktail of 2 antibodies.

Through two examples we demonstrate that the selectivity of the DuetMab for its target cell is determined by simultaneous

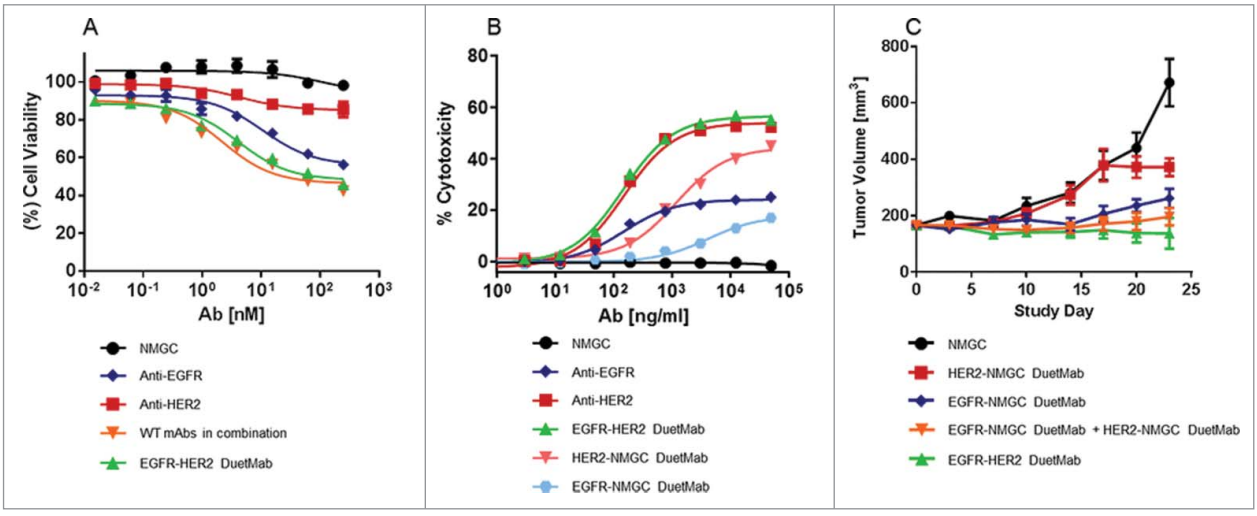

Figure 7. Biological activities of EGFR-HER2 DuetMab. (**A**) Viability of NCI-H358 cells. Each point represents the mean values of quadruplicate wells and the ± s.d. is represented by error bars. NMGC represents the control antibody. (**B**) ADCC assay with SK-OV3 cells. Each point represents the mean values of quadruplicate wells and the ± s.d. is represented by error bars. (**C**) Antitumor effect of EGFR-HER2 DuetMab and control molecules in nude mice bearing NCI-H358 xenografts. The mean values for each group are shown and the ± s.d. is represented by error bars.

Table 6. Pharmacokinetic analysis of EGFR-HER2 DuetMab and parental IgGs in human fcRn transgenic and SCID mice

Antibody	Mouse strain	Dose mg/kg	Cmax μg/ml	AUC μg*day/ml	T1/2 day	CL ml/day/kg	Vss ml/kg
Anti-EGFR IgG	hFcRn Tg	2.5	29 ± 4	67 ± 14	2.6 ± 0.5	39 ± 7	139 ± 22
Anti-EGFR IgG	SCID	10	126 ± 10	2120 ± 269	11.1 ± 1.6	5 ± 1	77 ± 7
Anti-HER2 IgG	hFcRn Tg	2.5	28 ± 5	40 ± 8	1.6 ± 0.3	65 ± 15	132 ± 23
Anti-HER2 IgG	SCID	10	131 ± 8	2560 ± 116	12.9 ± 1.0	3.9 ± 0.2	73 ± 6
EGFR/HER2 DuetMab	hFcRn Tg	2.5	37 ± 4	75 ± 11	2.5 ± 0.6	34 ± 5	115 ± 10
EGFR/HER2 DuetMab	SCID	10	115 ± 8	2020 ± 248	11.5 ± 1.1	5 ± 1	83 ± 5

PK parameters were determined by non-compartmental analysis using model 201. C_{max}: peak concentration; AUC: the area under concentration; time curve: $T^1/_2$: terminal half-life; CL: clearance; Vss: volume in steady state.

engagement of both antigens on the surface of the same cell. This creates an avidity effect such that, at low concentrations, DuetMabs show high specificity for double-expressing cells. While this would be expected to be true for other monovalent bispecific antibodies, to the best of our knowledge we are the first to demonstrate concurrent binding of a monovalent bispecific antibody to both antigens on the same cell. Because EGFR and HER2 are expressed separately on several normal tissues, a combination treatment with cetuximab and trastuzumab can have toxicities as seen in monotherapy with each antibody.[33,34] Because DuetMab exhibits better selectivity for cells expressing both the antigens compared to cells expressing one or the other antigen, we expect EGFR-HER2 DuetMab to have a favorable toxicity profile compared to a combination of cetuximab and trastuzumab. However, this can only be evaluated through further studies in non-human primates. Finally, although in this study we have demonstrated the principle of the DuetMab technology using antibodies directed against 2 different pairs of membrane receptors, we have so far generated 32 other DuetMabs against soluble targets and combinations of membrane and soluble targets. Most of these DuetMabs comprised of either Vκ or Vλ on both Fab arms or combinations of Vκ and Vλ. In total 16 different germlines for VH and 15 different germlines for VL have been tested in the DuetMab format. Also a few of the DuetMabs were made with mouse VH and Vκ belonging to 3 different germline genes for each chain (**Table S4**). In each case the expression levels, biophysical and biochemical properties were similar to the parental antibodies, much like what we have seen with the EGFR-HER2 and CD4-CD70 DuetMabs. The combined results from all the studies lead us to conclude that, because the DuetMab platform (i) does not involve V-domain engineering and is applicable over a wide range of different germline genes, (ii) reliably creates HC-LC heterodimerization when coupled to a HC dimerization technology such as KIH and (iii) is compatible with κ and λ isotypes it should be a generic platform that can be widely applied to other antibodies for bio-pharmaceutical development of molecules where monovalent binding to targets offer distinct advantage. Although the studies presented here are done with transiently expressed DuetMab, we have preliminary positive results indicating that when the expression of the different chains are balanced, DuetMab antibodies can be produced from engineered stable cell lines at yields comparable to those of conventional IgG antibodies and we hope to report on this in the future.

Materials and Methods

Design of alternative cysteine in C_H1-C_L interface and generation of a benchmark and reference standard for measuring bispecificity

To ensure correct chain pairings in our monovalent bispecific IgG, we remodeled the C_H1-C_L interface of one pair of heavy and light chains. The other pair was left unaltered. For the engineered interface, the 2 cysteines in C_H1 and C_L that form the wild-type interchain disulfide bond were mutated to valines. A pair of new cysteines was introduced at a different location in the C_H1-C_L interface to form the engineered disulfide bond. The positions for the new pair of cysteines were selected by screening 3 different position pairs in the C_H1-C_L interface for CH1, Cκ and Cλ (**Table 1**). The position for these residues remains the same for both kappa (κ) and lambda (λ) constant domains. Two criteria[35] were used to identify pairs of amino acids in C_H1-C_L interface suitable for substitution to cysteines: (i) a distance of 5.0–7.0 Å between corresponding α-carbons, similar to that found in naturally occurring disulfide bridges and (ii) the β-carbons pointing toward each other with a distance of 4.0–5.0 Å. Variants carrying a native disulfide bridge in one C_H1-C_L interface and an alternative interchain disulfide in the other C_H1-C_L interface were screened for correct assembly as monovalent bispecific IgG antibodies by AlphaLISA. For heterodimerization of the 2 heavy chains we employed the KIH technology and the addition of the stabilizing disulfide bridge in C_H3.[36]

We used 2 in-house antibodies to establish the platform. One targeted RAGE and the other targeted IL-6. The HC for the RAGE antibody had the knob mutations[37] and the HC of the IL-6 antibody had the hole mutations in the C_H3.[37] The cysteines in the C_H1 and C_L of the anti-RAGE antibody were mutated to valines and a new pair of cysteines was introduced in separate constructs according to the positions shown in **Table 1**. The C_H1 and C_L of the anti-IL-6 antibody had wild-type sequences. To determine correct pairing of cognate heavy and light chains, plasmids coding for the anti-RAGE and anti-IL6 were expressed together and tested for bispecificity by concurrent binding to RAGE and IL-6 proteins in an AlphaLISA assay (described below). Briefly, simultaneous binding to IL-6 and RAGE antigens brought the donor and acceptor beads into close proximity, which resulted in a recordable signal.

Construction of pDuet-Heavy and pDuet-Light vectors for production of DuetMab antibodies in mammalian cells

A significant problem in the production of bispecific IgGs is the formation of by-products and difficulties of removing them. Two plasmids were used for DuetMab expression. The pDuet-Heavy is a bicistronic plasmid and codes for the 2 HCs. The first cassette in this plasmid codes for the HC with the hole mutations in C_H3, while the second expression cassette codes for the knob mutation in the C_H3 and the $F^{126}C$ mutation in the C_H1. Because non-stoichiometric expression of the 2 chains can lead to the formation of hole-homodimers and hole half-IgG byproducts,[13,14] 2 additional mutations were introduced into the hole containing C_H3 to facilitate selective purification of correctly assembled DuetMabs. Histidine 435 was mutated to arginine ($H^{435}R$) because this mutation is known to ablate protein A binding.[38] Because arginine 435 co-occur with phenylalanine 436 in human IgG3 we also changed the tyrosine at position 436 to phenylalanine ($Y^{436}F$) to minimize potential immunogenicity of the DuetMab molecules. These two mutations, referred to as "RF" enabled easy removal of hole-hole homodimers and hole half-IgG byproducts during protein A purification of DuetMabs. Likewise, the pDuet-Light vector, is a bicistronic plasmid and codes for the 2 LCs. The second LC codes for the $S^{121}C$ mutation in the C_L.

Expression and purification of DuetMab antibodies

Antibodies were produced by transient co-transfection of HEK293F cells with pDuet-Heavy and pDuet-Light expression vectors using 293fectin™ (Invitrogen) in serum-free Freestyle™ medium (Invitrogen) according to the supplier's recommended procedures. Cell culture supernatants were harvested 6 days after transfection, filtered through a 0.22 μm sterile filter and the concentration of antibodies in cell-culture supernatants was measured by protein A Biosensors on an Octet384 instrument (ForteBio) in accordance with the manufacturer's protocol. Antibodies were purified by protein A affinity chromatography using MabSelect SuRe resin (GE Healthcare) in accordance with the manufacturer's protocol and were subsequently buffer exchanged in PBS (pH 7.2). The concentrations of purified antibodies were determined by reading the absorbance at 280 nm using the theoretically determined extinction coefficient for that protein. Purity was assessed by SDS-PAGE, SEC and RP-HPLC and other analytical techniques as described below.

AlphaLISA for identification of best position in C_H1-C_L interface for engineering disulfide bond

All AlphaLISA reagents were from PerkinElmer. Incubation steps with AlphaLISA beads were performed under subdued lighting at room temperature. Assays were performed in white 96-well half-area OptiPlates. Antibody samples (Reference standard, benchmark, KIH bispecific and variants 1, 2 and 3) at 0.1 μg/ml were incubated with 10 nM FLAG-tagged RAGE and biotinylated IL-6 proteins and 40 μg/ml AlphaLISA anti-FLAG Acceptor beads in 1X AlphaLISA Immunoassay Buffer for 1 h at room temperature. This was followed by the addition of Streptavidin-coated AlphaLISA Donor beads at 400 μg/ml. The mixture was incubated for 30 min, after which the assay plates were read on an EnVision plate reader (PerkinElmer). The two AlphaLISA beads can be brought into proximity only by a true bispecific molecule. Therefore, the measure of the AlphaLISA signal was taken as a measurement of the bispecificity. Since the benchmark sample was purified by two-step affinity chromatography using RAGE and IL6 matrix, it is reasonable to assume that it has 2 distinct antigen binding specificity, and therefore the signal produced by it was arbitrarily taken to mean nearly 100% bispecificity.

Analytical size-exclusion chromatography

Protein samples at 100 μg/ml were applied onto a TSK-gel G3000SWxL column (Tosoh Biosciences) at ambient column temperature. The samples were eluted isocratically with a mobile phase composed of 0.1 M sodium phosphate, 0.1 M sodium sulfate and 0.05% sodium azide, pH 6.8 at a flow rate of 1.0 mL/min over 20 minutes using an Agilent 1200 HPLC system. Eluted protein was detected using UV absorbance at 280 nm.

LC-MS of intact, deglycosylated, reduced and papain-digested samples

The deglycosylation was carried out by treating the proteins with PNGase F (QA-Bio LLC) at pH 7.4 and Endoglycosidase F2 (Sigma-Aldrich) at pH 4.5. Papain digestion was performed in a solution of 8 μg/ml papain (Sigma-Aldrich) in presence of 0.5 mM cysteine, pH 7.0. An ACQUITY/Q-Tof Premier LC-MS system (Waters) was used for antibody analysis and identification. Each sample was injected onto a 2 × 150 mm PRLP-S polymer column (8 μm, 4000A, Michrom Bioresources) at 0.2 ml/min. Mobile phase A was 0.1% trifluoroacetic acid (TFA) in HPLC grade water. Mobile phase B was 0.1% TFA in acetonitrile. Except for the separation of intact molecules, for which a gradient of 20% B to 60% B for 60 min was used, all the separations were carried out with a gradient of 25% B to 45% B for 30 min. The final concentration of each protein sample was ~1 mg/ml, and 10 μl was used for loading into the column. The MS signals were deconvoluted with MaxEnt 1, part of MassLynx software of Waters, which was used to control the LC-MS system and collect data.

Lys-C Peptide mapping

Free thiol groups in the sample were first capped using 1 mM N-ethylmaleimide. The sample was then denatured in a solution of 6 M guanidine in phosphate buffer, pH 7.0 at 37°C for 30 min. The denatured solution was diluted 2.5-fold with 100 mM phosphate buffer containing 0.06 mM EDTA at pH 7.0. Endoproteinase Lys-C was added at a 1:10 enzyme:protein ratio and the reaction mixture was incubated at 37°C for 16 h. Additional Lys-C was added at a 1:10 enzyme:protein ratio and incubated for a further 4 h at 37°C. Following Lys-C digestion, half of each reaction mixture was reduced by adding DTT to a final concentration of 30 mM and incubating at 37°C for 15 min. The other half of the reaction mixture was prepared without reduction. The digested peptides were separated by RP-HPLC on a BEH300 C18 column (1.7 μm, 2.1 × 150 mm) and

analyzed by a UV detector and an on-line LTQ Orbitrap mass spectrometer (ThermoElectron). The RP-UPLC mobile phase A was 0.02% TFA in water and the mobile phase B was 0.02% TFA in acetonitrile. Samples were eluted using a gradient of increasing buffer B. Peptides were identified and analyzed by comparing the results from the non-reduced and reduced peptide maps. The sequence of each peptide was identified using MS and confirmed using MS-MS (peptide mass sequencing), based on the known sequence of the protein. Disulfide bonded peptides were confirmed by MS data as peptides that were present only in the non-reduced sample. Free thiols were calculated based on the areas of selected ion chromatogram (SIC) for N-ethylmaleimide-labeled peptide divided by the areas of the corresponding reduced peptide.

Structure determination

For structural studies, the DuetMab Fab carrying the alternative interchain disulfide bond between C^{126} of HC and C^{121} of LC was produced by transient expression in HEK293F cells, purified over a cation exchange column (HiTrap SP HP [GE, CT]) and polished on a size exclusion chromatography column (Superdex 75 10/300 GL). DuetMab Fab was concentrated to ~19 mg/ml in 10 mM Tris, pH 8.0 and 100 mM NaCl, and subjected to crystallization trials using the automated Phoenix robotic system (Art Robbins Instruments, CA). Crystals were obtained only after using seeds from an unrelated Fab. The crystal used for data collection was grown by the sitting drop vapor diffusion method with a reservoir solution (0.3 ml) containing 0.018 M of each of the following salt solutions $CaCl_2$, $CoCl_2$, and $CdCl_2$, 18% PEG 3350 and 5% glycerol. Drops consisting of 2.0 μl protein + 1.0 μl precipitant mixed with 100× diluted seed stock were set up at room temperature where crystals appeared within 3-7 days. The crystals were cryoprotected by soaking in well solution supplemented with increasing concentrations of glycerol (5% per step with 5 steps) to a final concentration of 30%, then flash cooled and stored in liquid nitrogen until data collection. One diffraction data set from a single crystal was collected at a wavelength of 0.97931 Å and temperature of 100 K at the IMCA-CAT 17ID beamline of the Advanced Photon Source of the Argonne National Laboratory (University of Chicago, Chicago, IL) equipped with a PILATUS 6M detector. The 0.5° images were collected with exposure time of 0.8 s per frame. Data were processed using the XDS[39] package. Data statistics are presented in **Table S3**. The best solution in molecular replacement was found when V_H-V_L and C_H1-C_L domain pairs were used as separate models. The structure was then refined with REFMAC5[40] using all data in the resolution range of 15 Å to 2.2 Å. Water molecules were placed in the electron density peaks within hydrogen bond distances from protein atoms. The refinement statistics are given in **Table S3**. All crystallographic calculations were performed with the CCP4 suite of programs.[23] Model building was carried out using the program "O."[41] Figures were prepared with PyMOL (Schrodinger). The atomic coordinates and structure factors of the DuetMab Fab were deposited with the Protein Data Bank under accession number 4UB0.

Differential scanning calorimetry analysis

DSC experiments were performed using a Microcal VP-DSC scanning microcalorimeter (Microcal). All solutions and samples used for DSC were filtered using a 0.22 μm filter and degassed prior to loading into the calorimeter. Antibodies used for the DSC studies were >98% monomeric as determined by analytical SEC. Prior to DSC analysis all samples were exhaustively dialyzed (at least 3 buffer exchanges) in 25 mM histidine-HCl (pH 6.0). Buffer from this dialysis was used as reference buffer for subsequent DSC experiments. Prior to sample measurement, baseline measurements (buffer versus buffer) were subtracted from the sample measurement. Dialyzed samples (at a concentration of 1 mg/ml) were added to the sample well and DSC measurements were performed at a 1°C/min scan rate. Data analysis and deconvolution were carried out using the Origin™ DSC software provided by Microcal. Deconvolution analysis was performed using a non-2-state model and best fits were obtained using 100 iteration cycles. The $T_{m,onset}$ is defined as the qualitative temperature at which the thermogram appears to have a nonzero slope,[42] The T_m is defined as the temperature at which half of the molecules in a set are unfolded, and is calculated as the temperature value corresponding to each peak maximum on the thermogram.[42]

Biochemical binding assays

Kinetic measurements to EGFR and HER2 proteins were measured by biolayer interferometry on an Octet384 instrument (ForteBio). Antibodies at 10 μg/ml in PBS pH 7.2, 3 mg/ml BSA, 0.05% (v/v) Tween 20 (assay buffer) were captured on anti-human IgG Fc capture (AHC) biosensors (ForteBio). The loaded biosensors were washed with assay buffer to remove any unbound protein before carrying out association and dissociation measurements with serial dilutions of EGFR or HER2 for the indicated times. Kinetic parameters (k_{on} and k_{off}) and affinities (K_D) were calculated from a non-linear fit of the data using the Octet384 software v.7.2.

Concurrent binding studies to EGFR and HER2 proteins were performed in 2 formats. In the first format, purified antibodies were loaded on AHC biosensors as described above and then subjected for sequential associations, first with HER2 at 150 nM followed by incubation with EGFR and HER2, each at 150 nM. A terminal dissociation was carried out by subsequent incubation in assay buffer. In the second format, streptavidin (SA) biosensors (ForteBio) were used to capture biotinylated antigens at 5 μg/ml in assay buffer. Following a washing step, the loaded biosensors were subjected to successive association and dissociation interactions, first with 150 mM of the antibodies and then with the alternate antigen at 150 nM.

Kinetic measurements to recombinant human FcRn and Fcγ receptors were performed on a surface plasmon resonance-based ProteOn XPR36 biosensor (Bio-Rad) using steady state equilibrium binding assay. Antibodies at 50 μg/ml were immobilized on a GLC chip surface in 10 mM Na acetate buffer, pH 5.0 (Bio-Rad). Serial dilutions of either Fcγ receptors in PBS, pH 7.4, 0.005% Tween 20 (v/v), 3 mM EDTA or human and cynomolgus FcRn in 50 mM sodium phosphate, pH 6.0, 150 mM NaCl were passed over the immobilized surface. Binding studies

were performed at room temperature, and equilibrium binding rates of each analyte were determined and used to calculate equilibrium dissociation constants (K_D).

Preferential binding assays

Binding properties of CD4-CD70 DuetMab were assessed using lymphocyte populations expressing only one or both of the target antigens. Improved selectivity was measured in a combined culture system in which each cell type could be identified by tracer dyes. $CD4^+CD70^+$ cells were labeled with CellTrace™ Violet (Invitrogen), $CD4^+CD70^-$ cells with eFluor® 670 (eBioscience), and $CD4^-CD70^+$ cells were left unstained. Cells at 1×10^6 were washed twice with FACS Buffer (Phosphate Buffered Saline pH 7.2, 2% FBS, 2 mM EDTA and 0.1% Sodium Azide), combined at 1:1:1 ratio and incubated with serial dilutions of CD4-CD70 DuetMab and incubated at 4°C for 3 h. After washing with FACS buffer, cell-bound antibody was detected with PE-labeled anti-human Fc_γ (Jackson ImmunoResearch). Analysis was performed on an LSR II (Becton Dickinson) instrument and results were analyzed with the FlowJo program. Based on physical properties (height, width and density) only single cells were gated for analysis. To determine concurrent engagement of 2 antigens by cell-bound DuetMab, each cell population was examined individually using biotinylated soluble CD4 and CD70 and analyzed by flow cytometry using BV421-streptavidin (Biolegend) to detect any free antigen binding arm in the cell-bound DuetMab.

Improved selectivity of EGFR-HER2 DuetMab was similarly assessed as above in a 1:1:1 mixed population of SK-OV3, SKBr3 and A431 cells. SK-OV3 and SKBr3 cells were prelabeled with CellTrace™ Violet and eFluor® 670 stain, respectively, and A431 was kept unlabeled. Quantitative analysis of receptor density on the 3 cell lines was performed with QIFIKIT (DAKO) according to the manufacturer's instructions. Briefly, 1×10^6 cells were incubated with anti-EGFR mouse mAb (BioLegend) or anti-HER2 mouse mAb (R&D Systems) at saturating concentrations of 10 μg/ml in FACS buffer for 1 h at 4°C. After washing twice with FACS buffer, AlexaFluor®488 -conjugated goat anti-mouse IgG F(ab)2 (Molecular Probes) at 20 μg/ml was added for 45 min at 4°C. Optimal primary and secondary antibody concentrations were determined by titration. QIFIKIT Bead standards coated with defined amounts of anti-CD5 mouse mAb were labeled in parallel under the same conditions described above. Data acquisition and analysis, including linear regression of the calibration curve and calculation of antigen density, was completed according to the manufacturer's instructions. The density of each of the 2 receptors on the cell lines were as follows: A431 (EGFR: $83.3 \times 10^4 \pm 5.2 \times 10^4$, HER2: $3.3 \times 10^4 \pm 0.15 \times 10^4$); SK-OV3 (EGFR:$14.4 \times 10^4 \pm 0.7 \times 10^4$, HER2: $34.5 \times 10^4 \pm 1.4 \times 10^4$) and SKBr3 (EGFR: $4.2 \times 10^4 \pm 0.3 \times 10^4$, HER2: $176 \times 10^4 \pm 7.2 \times 10^4$). To determine concurrent engagement of 2 antigens by cell-bound DuetMab, each cell population was examined individually using biotinylated soluble EGFR and HER2 and analyzed by flow cytometry using BV421-streptavidin (Biolegend) to detect any free antigen binding arm in the cell-bound DuetMab.

Cell viability assay

Cell viability was measured by the CellTiter-Glo® Luminescent Cell Viability Assay (Promega) kit. NCI-H358 cells were seeded in 96-well plates at a density of 5×10^3 cells/well in DMEM supplemented with 10% FCS. Antibodies at various concentrations were added to quadruplicate samples, and the cells were incubated for 96 h at 37°C in 5% CO_2 atmosphere. After treatment, the cells were exposed to the CellTiter-Glo® reagent for 20 min and the luminescent was measured using an EnVision plate reader (PerkinElmer). The IC_{50} values were defined as the antibody concentrations inhibiting cell growth by 50%.

ADCC assay

ADCC activities were measured by the CytoTox 96 Non-Radioactive Cytotoxicity Assay (Promega) kit. SK-OV3 cells were seeded in 96-well plates at a density of 2×10^4 cells/well in RPMI-1640 without phenol red and supplemented with 5% FBS. A human NK cell line (KC1333) from a malignant non-Hodgkin's lymphoma transgenic for human CD16 (FcγRIIIA) and FcεRIγ (Xellerex/Biowa) were mixed with target cells at an E:T ratio of 2.5:1. Antibodies at various concentrations were added to quadruplicate samples, and the cells were incubated for 16 h at 37°C in 5% CO_2 atmosphere. After treatment, the cells were exposed to the CytoTox 96 reagent for 30 min and OD at 490 nm was measured using a Spectramax 340PC plate reader.

Antitumor activity assay

NCI-H358 cells were implanted subcutaneously into the right flank of 5–7 week old female athymic nude mice (Harlan). Tumors were allowed to reach approximately 160 mm^3 when mice with a uniform tumor volume were sorted into study groups of 10 animals each. Different groups were treated twice a week, intraperitonially, with one of the following: 5 mg/kg of EGFR-HER2 DuetMab, EGFR-NMGC DuetMab, HER2-NMGC DuetMab; a combination of EGFR-NMGC DuetMab and HER2-NMGC DuetMab each at (5 mg/kg); and parental NMGC IgG as a negative control. Tumors were measured at 3 day intervals with calipers and tumor volume was calculated as $[L(\text{length}) \times W^2(\text{width})]/2$.

Pharmacokinetic analysis

Eight-week-old female SCID and human FcRn transgenic mice (Jackson Laboratory, Tg276, hemizygous for huFcRn, ref. [26]) were injected intravenously with transtuzumab, cetuximab or EGFR-HER2 DuetMab at a dose of 10 mg/kg and 2.5 mg/kg, respectively. Approximately 150 μl of blood was collected retro-orbitally at different time points. At the last time point blood was collected by cardiac puncture before mice were terminated. The concentration of human antibodies in the serum was determined by ELISA. Mouse anti-human IgG Fc fragment specific antibody (Jackson ImmunoResearch) was used to capture the human antibodies from serum samples and goat anti-human Fab conjugated with horse radish peroxidase (Sigma) was used for detection. Plates were read on an EnVision plate reader (PerkinElmer) and the pharmacokinetic parameters were obtained by non-compartmental analysis using model 201.

Disclosure of Potential Conflicts of Interest

No potential conflicts of interest were disclosed.

Supplemental Material

Supplemental data for this article can be accessed on the publisher's website.

References

1. Kontermann RE. Alternative antibody formats. Curr Opin Mol Ther 2010; 12:176-83; PMID:20373261
2. Kontermann R. Dual targeting strategies with bispecific antibodies. MAbs 2012; 4:182-97; PMID:22453100; http://dx.doi.org/10.4161/mabs.4.2.19000
3. Chan AC, Carter PJ. Therapeutic antibodies for autoimmunity and inflammation. Nat Rev Immunol 2010; 10:301-16; PMID:20414204; http://dx.doi.org/10.1038/nri2761
4. Marvin JS, Zhu Z. Recombinant approaches to IgG-like bispecific antibodies. Acta Pharmacol Sin 2005; 26:649-58; PMID:15916729; http://dx.doi.org/10.1111/j.1745-7254.2005.00119.x
5. Thakur A, Lum LG. Cancer therapy with bispecific antibodies: clinical experience. Curr Opin Mol Ther 2010; 12:340-9; PMID:20521223
6. Demarest SJ, Hariharan K, Dong J. Emerging antibody combinations in oncology. MAbs 2011; 3:338-51; PMID:21697653; http://dx.doi.org/10.4161/mabs.3.4.16615
7. Klein C, Sustmann C, Thomas M, Stubenrauch K, Croasdale R, Schanzer J, Brinkmann U, Kettenberger H, Regula JT, Schaefer W. Progress in overcoming the chain association issue in bispecific heterodimeric IgG antibodies. MAbs 2012; 4:653-63; PMID:22925968; http://dx.doi.org/10.4161/mabs.21379
8. Pacchiana G, Chiriaco C, Stella MC, Petronzelli F, De Santis R, Galluzzo M, Carminati P, Comoglio PM, Michieli P, Vigna E. Monovalency unleashes the full therapeutic potential of the DN-30 anti-met antibody. J Biol Chem 2010; 285:36149-57; PMID:20833723; http://dx.doi.org/10.1074/jbc.M110.134031
9. Ridgway JB, Presta LG, Carter P. ';Knobs-into-holes' engineering of antibody CH3 domains for heavy chain heterodimerization. Protein Eng 1996; 9:617-21; PMID:8844834; http://dx.doi.org/10.1093/protein/9.7.617
10. Gunasekaran K, Pentony M, Shen M, Garrett L, Forte C, Woodward A, Ng SB, Born T, Retter M, Manchulenko K, et al. Enhancing antibody Fc heterodimer formation through electrostatic steering effects: applications to bispecific molecules and monovalent IgG. J Biol Chem 2010; 285:19637-46; PMID:20400508; http://dx.doi.org/10.1074/jbc.M110.117382
11. Davis JH, Aperlo C, Li Y, Kurosawa E, Lan Y, Lo KM, Huston JS. SEEDbodies: fusion proteins based on strand-exchange engineered domain (SEED) CH3 heterodimers in an Fc analogue platform for asymmetric binders or immunofusions and bispecific antibodies. Protein Eng Des Sel 2010; 23:195-202; PMID:20299542; http://dx.doi.org/10.1093/protein/gzp094
12. Christensen EH, Eaton DL, Vendel AC, Wranik B. Coiled coil and/or tether containing protein complexes and uses thereof. 2011. WO/2011/034605.
13. Merchant AM, Zhu Z, Yuan JQ, Goddard A, Adams CW, Presta LG, Carter P. An efficient route to human bispecific IgG. Nat Biotechnol 1998; 16:677-81; PMID:9661204
14. Schaefer W, Regula JT, Bahner M, Schanzer J, Croasdale R, Durr H, Gassner C, Georges G, Kettenberger H, Imhof-Jung S, et al. Immunoglobulin domain crossover as a generic approach for the production of bispecific IgG antibodies. Proc Natl Acad Sci U S A 2011; 108:11187-92; PMID:21690412; http://dx.doi.org/10.1073/pnas.1019002108
15. Wranik BJ, Christensen EL, Schaefer G, Jackman JK, Vendel AC, Eaton D. LUZ-Y, a novel platform for the mammalian cell production of full-length IgG-bispecific antibodies. J Biol Chem 2012; 287:43331-9; PMID:23118228; http://dx.doi.org/10.1074/jbc.M112.397869
16. Strop P, Ho WH, Boustany LM, Abdiche YN, Lindquist KC, Farias SE, Rickert M, Appah CT, Pascua E, Radcliffe T, et al. Generating bispecific human IgG1 and IgG2 antibodies from any antibody pair. J Mol Biol 2012; 420:204-19; PMID:22543237; http://dx.doi.org/10.1016/j.jmb.2012.04.020
17. Spiess C, Merchant M, Huang A, Zheng Z, Yang NY, Peng J, Ellerman D, Shatz W, Reilly D, Yansura DG, et al. Bispecific antibodies with natural architecture produced by co-culture of bacteria expressing two distinct half-antibodies. Nat Biotechnol 2013; 31:753-58; PMID:23831709; http://dx.doi.org/10.1038/nbt.2621
18. Lewis SM, Wu X, Pustilnik A, Sereno A, Huang F, Rick HL, Guntas G, Leaver-Fay A, Smith EM, Ho C, et al. Generation of bispecific IgG antibodies by structure-based design of an orthogonal Fab interface. Nat Biotechnol 2014; 32:191-8; PMID:24463572; http://dx.doi.org/10.1038/nbt.2797
19. Schanzer JM, Wartha K, Croasdale R, Moser S, Kunkele KP, Ries C, Scheuer W, Duerr H, Pompiati S, Pollman J, et al. A novel glycoengineered bispecific antibody format for targeted inhibition of epidermal growth factor receptor (EGFR) and insulin-like growth factor receptor type I (IGF-1R) demonstrating unique molecular properties. J Biol Chem 2014; 289:18693-706; PMID:24841203; http://dx.doi.org/10.1074/jbc.M113.528109
20. Bostrom J, Yu SF, Kan D, Appleton BA, Lee CV, Billeci K, Man W, Peale F, Ross S, Wiesmann C, et al. Variants of the antibody herceptin that interact with HER2 and VEGF at the antigen binding site. Science 2009; 323:1610-4; PMID:19299620; http://dx.doi.org/10.1126/science.1165480
21. Rouet R, Christ D. Bispecific antibodies with native chain structure. Nat Biotechnol 2014; 32:136-7; PMID:24509759; http://dx.doi.org/10.1038/nbt.2812
22. McCoy AJ, Grosse-Kunstleve RW, Adams PD, Winn MD, Storoni LC, Read RJ. Phaser crystallographic software. J Appl Crystallogr 2007; 40:658-74; PMID:19461840; http://dx.doi.org/10.1107/S0021889807021206
23. Bailey S. The CCP4 suite - programs for protein crystallography. Acta Crystallogr Sect D-Biol Crystallogr 1994; 50:760-3; PMID:15299452; http://dx.doi.org/10.1107/S0907444993011898
24. Cho HS, Mason K, Ramyar KX, Stanley AM, Gabelli SB, Denney DW Jr, Leahy DJ. Structure of the extracellular region of HER2 alone and in complex with the Herceptin Fab. Nature 2003; 421:756-60; PMID:12610629; http://dx.doi.org/10.1038/nature01392
25. Roopenian DC, Christianson GJ, Sproule TJ. Human FcRn transgenic mice for pharmacokinetic evaluation of therapeutic antibodies. Methods Mol Biol 2010; 602:93-104; PMID:20012394; http://dx.doi.org/10.1007/978-1-60761-058-8_6
26. Andersen JT, Daba MB, Berntzen G, Michaelsen TE, Sandlie I. Cross-species binding analyses of mouse and human neonatal Fc receptor show dramatic differences in immunoglobulin G and albumin binding. J Biol Chem 2010; 285:4826-36; PMID:20018855; http://dx.doi.org/10.1074/jbc.M109.081828
27. Brabender J, Danenberg KD, Metzger R, Schneider PM, Park J, Salonga D, Hölscher AH, Danenberg PV. Epidermal growth factor receptor and HER2-neu mRNA expression in non-small cell lung cancer is correlated with survival. Clin Cancer Res 2001; 7:1850-5; PMID:11448895
28. Carlsson J, Shen L, Xiang J, Xu J, Wei Q. Tendencies for higher co-expression of EGFR and HER2 and downregulation of HER3 in prostate cancer lymph node metastases compared with corresponding primary tumors. Oncol Lett 2013; 5:208-14; PMID:23255921
29. Quesnelle KM, Grandis JR. Dual kinase inhibition of EGFR and HER2 overcomes resistance to cetuximab in a novel in vivo model of acquired cetuximab resistance. Clin Cancer Res 2011; 17:5935-44; PMID:21791633; http://dx.doi.org/10.1158/1078-0432.CCR-11-0370
30. Larbouret C, Robert B, Navarro-Teulon I, Thezenas S, Ladjemi MZ, Morisseau S, Campigna E, Bibeau F, Mach JP, Pèlegrin A, et al. In vivo therapeutic synergism of anti-epidermal growth factor receptor and anti-HER2 monoclonal antibodies against pancreatic carcinomas. Clin Cancer Res 2007; 13:3356-62; PMID:17545543; http://dx.doi.org/10.1158/1078-0432.CCR-06-2302
31. Kawaguchi Y, Kono K, Mimura K, Mitsui F, Sugai H, Akaike H, Fujii H. Targeting EGFR and HER-2 with cetuximab- and trastuzumab-mediated immunotherapy in oesophageal squamous cell carcinoma. Br J Cancer 2007; 97:494-501; PMID:17622245; http://dx.doi.org/10.1038/sj.bjc.6603885
32. Larbouret C, Robert B, Bascoul-Mollevi C, Penault-Llorca F, Ho-Pun-Cheung A, Morisseau S, Navarro-Teulon I, Mach JP, Pèlegrin A, Azria D. Combined cetuximab and trastuzumab are superior to gemcitabine in the treatment of human pancreatic carcinoma xenografts. Ann Oncol 2010; 21:98-103; PMID:19889608; http://dx.doi.org/10.1093/annonc/mdp496
33. Saif MW, Kim R. Incidence and management of cutaneous toxicities associated with cetuximab. Expert Opin Drug Safety 2007; 6:175-82; PMID:17367263; http://dx.doi.org/10.1517/14740338.6.2.175
34. Ewer MS, O'Shaughnessy JA. Cardiac toxicity of trastuzumab-related regimens in HER2-overexpressing breast cancer. Clin Breast Cancer 2007; 7:600-7; PMID:17592672; http://dx.doi.org/10.3816/CBC.2007.n.017
35. Srinivasan N, Sowdhamini R, Ramakrishnan C, Balaram P. Conformations of disulfide bridges in proteins. Int J Pept Protein Res 1990; 36:147-55; PMID:2272751; http://dx.doi.org/10.1111/j.1399-3011.1990.tb00958.x
36. Atwell S, Ridgway JB, Wells JA, Carter P. Stable heterodimers from remodeling the domain interface of a homodimer using a phage display library. J Mol Biol 1997; 270:26-35; PMID:9231898; http://dx.doi.org/10.1006/jmbi.1997.1116
37. Carter P. Bispecific human IgG by design. J Immunol Methods 2001; 248:7-15; PMID:11223065; http://dx.doi.org/10.1016/S0022-1759(00)00339-2
38. Jendeberg L, Nilsson P, Larsson A, Denker P, Uhlen M, Nilsson B, Nygren PA. Engineering of Fc(1) and Fc (3) from human immunoglobulin G to analyse subclass specificity for staphylococcal protein A. J Immunol Methods 1997; 201:25-34; PMID:9032407; http://dx.doi.org/10.1016/S0022-1759(96)00215-3
39. Kabsch W. XDS. Acta Crystallogr Section D, Biol Crystallogr 2010; 66:125-32; PMID:20124692; http://dx.doi.org/10.1107/S0907444909047337
40. Murshudov GN, Skubak P, Lebedev AA, Pannu NS, Steiner RA, Nicholls RA, Winn MD, Long F, Vagin AA. REFMAC5 for the refinement of macromolecular crystal structures. Acta Crystallogr Section D, Biol Crystallogr 2011; 67:355-67; PMID:21460454; http://dx.doi.org/10.1107/S0907444911001314
41. Jones TA, Zou JY, Cowan SW, Kjeldgaard M. Improved methods for building protein models in electron density maps and the location of errors in these models. Acta Crystallogr Section A, Found Crystallogr 1991; 47 (Pt 2):110-9; PMID:2025413; http://dx.doi.org/10.1107/S0108767390010224
42. Beckley NS, Lazzareschi KP, Chih HW, Sharma VK, Flores HL. Investigation into temperature-induced aggregation of an antibody drug conjugate. Bioconjugate Chem 2013; 24:1674-83; PMID:24070051; http://dx.doi.org/10.1021/bc400182x